Radiolabeling of a polypeptide polymer for intratumoral delivery of alpha-particle emitter, 225Ac, and beta-particle emitter, 177Lu

Shalgunov, V.; Engudar, G.; Bohrmann, L.; Wharton, L.; Maskell, K.; Johann, K.; ... ; Radchenko, V.

Nuclear Medicine and Biology 104–105 (2022) 11–21

Contents lists available at ScienceDirect

Nuclear Medicine and Biology

journal homepage: www.elsevier.com/locate/nucmedbio

Radiolabeling of a polypeptide polymer for intratumoral delivery of alpha-particle emitter, ^{225}Ac, and beta-particle emitter, ^{177}Lu

Vladimir Shalgunov [a,1], Gokce Engudar [b,1], Lennart Bohrmann [a,c], Luke Wharton [b,d], Keiran Maskell [b,e], Kerstin Johann [f], Matthias Barz [f,g], Paul Schaffer [b,e,h], Matthias M. Herth [a,i,**], Valery Radchenko [b,j,*]

[a] Department for Drug Design and Pharmacology, Faculty of Health and Medical Sciences, University of Copenhagen, Universitetsparken 2, 2100 Copenhagen, Denmark
[b] Life Sciences Division, TRIUMF, 4004 Wesbrook Mall, Vancouver, BC V6T 2A3, Canada
[c] Faculty of Pharmaceutical Sciences, University of British Columbia, 2405 Wesbrook Mall, Vancouver, BC V6T 1Z3, Canada
[d] Medicinal Inorganic Chemistry Group, Department of Chemistry, University of British Columbia, 2036 Main Mall, Vancouver, BC V6T 1Z, Canada
[e] Department of Chemistry, Simon Fraser University, 8888 University Drive, Burnaby, BC V5A 0A7, Canada
[f] Department of Chemistry, Johannes Gutenberg University, Duesbergweg 10-14, 55128 Mainz, Germany
[g] Division of Biotherapeutics, Leiden Academic Center for Drug Research (LACDR), Einsteinweg 55, 2333CC Leiden, the Netherlands
[h] Department of Radiology, University of British Columbia, 2775 Lauret St, Vancouver, BC V5Z 1M9, Canada
[i] Department of Clinical Physiology, Nuclear Medicine & PET, Rigshospitalet, Blegdamsvej 9, 2100 Copenhagen, Denmark
[j] Department of Chemistry, University of British Columbia, 2036 Main Mall, Vancouver, BC V6T 1Z, Canada

ARTICLE INFO

Article history:
Received 30 July 2021
Received in revised form 22 October 2021
Accepted 8 November 2021

Available online xxxx

Keywords:
Targeted radionuclide therapy
Tetrazine ligation
^{177}Lu
^{225}Ac
Polyglutamic acid
Polypeptides

ABSTRACT

Introduction: Radiotherapy of cancer requires both alpha- and beta-particle emitting radionuclides, as these radionuclide types are efficient at destroying different types of tumors. Both classes of radionuclides require a vehicle, such as an antibody or a polymer, to be delivered and retained within the tumor. Polyglutamic acid (pGlu) is a polymer that has proven itself effective as a basis of drug-polymer conjugates in the clinic, while its derivatives have been used for pretargeted tumor imaging in a research setup. *trans*-Cyclooctene (TCO) modified pGlu is suitable for pretargeted imaging or therapy, as well as for intratumoral radionuclide therapy. In all cases, it becomes indirectly radiolabeled via the bioorthogonal click reaction with the tetrazine (Tz) molecule carrying the radionuclide. In this study, we report the radiolabeling of TCO-modified pGlu with either lutetium-177 (^{177}Lu), a beta-particle emitter, or actinium-225 (^{225}Ac), an alpha-particle emitter, using the click reaction between TCO and Tz.
Methods: A panel of Tz derivatives containing a metal ion binding chelator (DOTA or macropa) connected to the Tz moiety directly or through a polyethylene glycol (PEG) linker was synthesized and tested for their ability to chelate ^{177}Lu and ^{225}Ac, and click to pGlu-TCO. Radiolabeled ^{177}Lu-pGlu and ^{225}Ac-pGlu were isolated by size exclusion chromatography. The retention of ^{177}Lu or ^{225}Ac by the obtained conjugates was investigated *in vitro* in human serum.
Results: All DOTA-modified Tzs efficiently chelated ^{177}Lu resulting in average radiochemical conversions (RCC) of >75%. Isolated radiochemical yields (RCY) for ^{177}Lu-pGlu prepared from ^{177}Lu-Tzs ranged from 31% to 55%. TLC analyses detected <5% unchelated ^{177}Lu for all ^{177}Lu-pGlu preparations over six days in human serum. For ^{225}Ac chelation, optimized RCCs ranged from 61 ± 34% to quantitative for DOTA-Tzs and were quantitative for the macropa-modified Tz (>98%). Isolated radiochemical yields (RCY) for ^{225}Ac-pGlu prepared from ^{225}Ac-Tzs ranged from 28% to 51%. For 3 out of 5 ^{225}Ac-pGlu conjugates prepared from DOTA-Tzs, the amount of unchelated ^{225}Ac stayed below 10% over six days in human serum, while ^{225}Ac-pGlu prepared from macropa-Tz showed a steady release of up to 37% ^{225}Ac.
Conclusion: We labeled TCO-modified pGlu polymers with alpha- and beta-emitting radionuclides in acceptable RCYs. All ^{177}Lu-pGlu preparations and some ^{225}Ac-pGlu preparations showed excellent stability in human plasma. Our work shows the potential of pGlu as a vehicle for alpha- and beta-radiotherapy of tumors and demonstrated the usefulness of Tz ligation for indirect radiolabeling.

* Correspondence to: V. Radchenko, Life Sciences Division, TRIUMF, 4004 Wesbrook Mall, Vancouver, BC V6T 2A3, Canada.
** Correspondence to: M.M. Herth, Department for Drug Design and Pharmacology, Faculty of Health and Medical Sciences, University of Copenhagen, Universitetsparken 2, 2100 Copenhagen, Denmark.
E-mail addresses: matthias.herth@sund.ku.dk (M.M. Herth), vradchenko@triumf.ca (V. Radchenko).
[1] These authors contributed equally.

https://doi.org/10.1016/j.nucmedbio.2021.11.001
0969-8051/

1. Introduction

Radionuclide therapy is used for the treatment of cancer by delivering a therapeutic radiation dose to malignant tissues either by means of targeted delivery using intravenously injected vehicles like antibodies, peptides or nanoparticles (i.e. targeted radionuclide therapy (TRT)) [1,2], or by directly implanting a sealed radioactive source in or near the tumor (i.e., brachytherapy (BT)) [3].

The therapeutic radiation dose for radionuclide therapy is typically delivered by beta- or alpha-particle emitting radionuclides, which differ in the mean tissue range and linear energy transfer (LET) of their emitted particles. Beta-emitting radionuclides are characterized by a comparatively long mean tissue range in the order of 1–5 mm and a low LET of ~0.2 keV/μm. Among beta-particle emitting therapeutic radionuclides (i.e., ^{90}Y, ^{131}I, ^{153}Sm, ^{177}Lu, ^{186}Re), the use of ^{177}Lu has attracted a growing interest for the development of radiopharmaceuticals, owing to its suitable decay characteristics and the possibility of theranostic imaging by Single-Photon Emission Computed Tomography (SPECT) (Table 1) [4]. ^{177}Lu is able to provide uniform dose distribution due to the cross-fire effect of beta-particles which is advantageous for the irradiation of small heterogeneous tumors [5–7]. In contrast, alpha-particles have a much higher LET (approx. 80–100 keV/μm) with a short mean tissue range of 40–100 μm which makes it effective for the treatment of small metastatic lesions and single-cell metastatic diseases [2,8]. This high density ionization over a short path leads to irreparable DNA double strand breaks and an increased cytotoxicity irrespective of tissue oxygenation, while preventing damage to the surrounding healthy tissue [9]. Alpha-particles could complement therapies with beta-particles and could be also used as a therapeutic adjuvant [10,11]. ^{225}Ac is one of the most effective alpha-emitting radionuclides for TRT by virtue of its favorable decay characteristics (e.g., half-life, rapid and successive emission of four alpha and two beta-particles through its decay chain, and emission energy) (Table 1) [12]. Despite the promising physical characteristics of ^{225}Ac, its use in TRT has been limited by a number of challenges including insufficient availability and limited radiochemistry development and a paucity of available bifunctional chelators for the complexation of ^{225}Ac for covalent incorporation onto molecular delivery vehicles [13]. In this work, ^{225}Ac derived from the decay of ^{229}Th was used provided through collaboration with Canadian Nuclear Laboratories (CNL) [14]. In addition to this effort in CNL, TRIUMF has successfully produced ^{225}Ac via several production routes (e.g., the separation of ^{225}Ra and ^{225}Ac generated from ISAC beam, proton spallation of ^{232}Th target) to make it accessible for the development of ^{225}Ac-based radiopharmaceuticals [13,15].

Bifunctional chelators are essential components of metal-based radiopharmaceuticals that are able to form a stable complex with a metallic radioisotope and tether it to a carrier molecule. The well-known 1,4,7,10-tetraazacyclododecane-1,4,7,10-tetraacetic acid (DOTA) chelator has previously been used for the synthesis of ^{225}Ac radioimmunoconjugates [18,19]. However, the chelation of DOTA to large $^{225}Ac^{3+}$ ion is kinetically slow and requires high chelator concentration and elevated temperatures to yield in sufficient radiolabeling [8]. Several other macrocyclic chelators (e.g., HEHA, H_2macropa, H_4py4pa, crown) have been also synthesized for the chelation of ^{225}Ac and evaluated *in vivo* for their stability and biodistribution [20–23]. Among those, macropa was able to form stable complexes with ^{225}Ac within 5 min at room temperature [21].

An indirect labeling approach based on the bioorthogonal inverse electron-demand Diels–Alder (IEDDA) reaction has been developed. IEDDA involves a reaction between 1,2,4,5-tetrazine (Tz) and the dienophile, *trans*-cyclooctene (TCO), and has shown promising results for the labeling of biomolecules with a variety of radioisotopes and has been successfully applied for *in vivo* pretargeted imaging [24–26], radioimmunotherapy [27–29] and radiolabeling of antibodies and peptides [30–33]. Briefly, in this approach a bifunctional chelator is covalently appended to Tz and labeled with a radioisotope. Subsequently, the labeled Tz-chelator conjugate is reacted with TCO-modified polypeptides under mild conditions to afford the radiolabeled macromolecule [30,32,34]. This strategy has been applied both for traditional radiolabeling as well as for *in vivo* pretargeting. Poty et al. evaluated this strategy for the labeling of two antibodies with DOTA-functionalized Tzs for the complexation of ^{225}Ac and reported higher radiochemical yield and molar activities compared to direct labeling approaches of antibodies with ^{225}Ac [35].

For internal radionuclide therapy via intratumoral injection of radionuclides, effective encapsulation of therapeutic radionuclides is needed for deposition of therapeutic radiation in the tumor, while minimizing side effects to healthy tissue. For this purpose, several delivery vehicles including polymers [36–38], lipid nanoparticles [39,40], nanogel formulations [41], or gold nanoparticles [42] have been investigated to enable intratumoral administration of radionuclides (e.g., ^{90}Y, ^{131}I, ^{186}Re, ^{177}Lu, ^{103}Pd).

The highly biocompatible and biodegradable poly(α-glutamic acid) (pGlu) can be synthesized by controlled ring opening polymerization of the corresponding α-amino acid-N-carboxy anhydride by using various initiators, ammonium salts, or ultra pure reagents with precise control over molecular weight [43–45]. It has been already used for the design of polymer drug conjugates (e.g., Opaxio™), which entered clinical studies for the treatment of several cancer types [46,47]. In recent studies, pGlu has been functionalized with reactive groups, such as TCO, to allow for site-selective conjugation of bioactive molecules and *in vivo* bioorthogonal ligation [48,49]. We previously showed that TCO-modified pGlu reacted with ^{11}C-labeled tetrazine was stably retained in the tumor after intratumoral injection [49]. We also reported rapid *in vivo* ligation kinetics and SPECT imaging of a bifunctional DOTA-Tz and a pGlu polymer modified with polysarcosine (pSar) strands with improved pharmacokinetic properties [50]. These results encouraged us to further explore pGlu-based injectable polymers as vehicles for the delivery of therapeutic radionuclides ^{177}Lu and ^{225}Ac into the tumor.

In this work, we examined the radiolabeling of pGlu with ^{177}Lu and ^{225}Ac using the IEDDA reaction between TCO-modified pGlu and radiolabeled Tz chelates (Fig. 1). Five Tz constructs containing the heptadentate (**1**–**3**) or octadentate (**4** and **5**) DOTA chelator (Fig. 2) were prepared and radiolabeled with ^{177}Lu and ^{225}Ac. We hypothesized that octadentate DOTA derivatives would provide greater chelation efficiency or superior stability compared to heptadentate analogs. In structures **1** and **4**, where the Tz and DOTA moieties connected without a spacer, these moieties might exert a negative influence on each other's reactivity. To control this potential risk, a polyethylene glycol (PEG) linker was inserted into the structures of **1** and **4** to yield compounds

Table 1
Decay characteristics of the radionuclides used in this study [4,16,17].

Radionuclide	Decay mode	Emission energy (E_{mean})	Gamma photons energy (E_γ)	Half-life (days)	Penetration range in tissue (mm)
$^{177}Lu^{3+}$	β^- emission	134 keV	209 keV (11%), 113 keV (6.4%)	6.65	<2
$^{225}Ac^{3+}$	4 α and 2 β^- emission	5.8 MeV (^{225}Ac, 50.7%), 6.3 MeV (^{221}Fr, 83.3%), 7.1 MeV (^{217}At, 99.9%), 5.9 MeV (^{213}Bi, 2%)	440 keV (^{213}Bi, 26%) 217 keV (^{221}Fr, 11%)	9.92	0.047–0.085

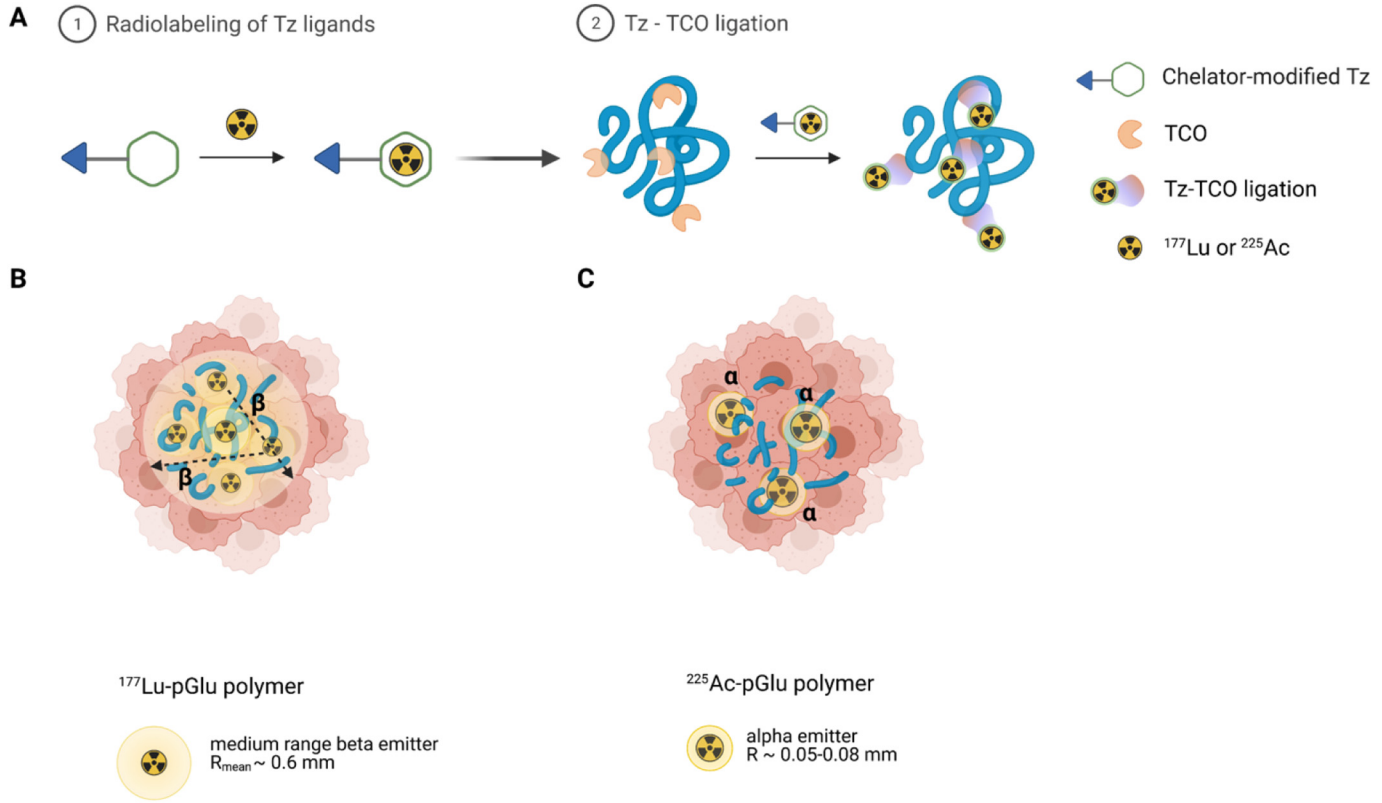

Fig. 1. Schematic illustration of ^{177}Lu or ^{225}Ac-labeled pGlu polymer for alpha- or beta- therapy of tumors. (A) Radiolabeling workflow to obtain ^{177}Lu-pGlu or ^{225}Ac-pGlu. (B) Homogeneous and diffuse distribution of the therapeutic dose in the tumor expected for ^{177}Lu-pGlu with a maximum tissue penetration depth of 2 mm (R_{mean} ~ 0.5–0.6). (C) Heterogeneous and localized distribution of the therapeutic dose in the tumor expected for ^{225}Ac-pGlu with a tissue penetration depth range 47–85 μm.

2 and **5**, respectively. In addition to methyl-substituted Tzs (**1**, **2**, **4**, and **5**), we selected a bispyridyl-substituted Tz derivative **3** with an ultra-long PEG linker for the current study. Radiolabeling of **3** with several radioisotopes (e.g., ^{111}In, ^{177}Lu, ^{68}Ga, ^{44}Sc) was previously reported to result in quantitative radiochemical conversions, and radiolabeled **3** showed fast and efficient *in vivo* click reactivity to TCO-functionalized macromolecules [51–55]. Finally, a linker-free macropa-conjugated Tz (**6**) was studied for the chelation of ^{225}Ac (Fig. 2).

The workflow if this study was as follows. First, ^{177}Lu or ^{225}Ac-labeled Tz constructs were prepared by chelation of the respective radiometals. Second, the radiolabeled Tz derivatives were allowed to react with the TCO-modified pGlu. Radiometal chelation efficiencies and the obtained yields of radiolabeled pGlu conjugates for different Tz chelates were compared. Finally, the stability of the purified radiolabeled pGlu preparations in human serum was evaluated.

2. Materials and methods

2.1. General

All reactions involving dry solvents or sensitive agents were performed under an anhydrous nitrogen atmosphere and dried glassware prior to use. Commercially available chemicals were used as received. Solvents were dried prior to use with an SG water solvent purification system or dried using standard procedures. The ^{1}H NMR spectra were recorded on a 400 MHz Avance III or 600 MHz Avance III HD (Bruker, Bremen, Germany). Analytical HPLC was performed using an UltiMate HPLC system consisting of an LPG-3400A pump (1 mL/min), a WPS-3000SL autosampler, and a 3000 Diode Array Detector installed with a Gemini-NX C18 (250 × 4.60 mm, 3 μm) column. Solvent A: H_2O + 0.1% TFA; Solvent B: MeCN-H_2O 9:1 + 0.1% TFA. For HPLC control, data collection and data handling, Chromeleon software v. 6.80 was used. Preparative HPLC was carried out on an Ultimate Thermo SCIENTIFIC HPLC system with an LPG-3200BX pump, a Rheodyne 9721i injector, a 10 mL loop, an MWD-3000SD detector (200, 210, 225 and 254 nm), and a Gemini-NX C18 (250 × 21.2 mm, 5 μm) column. Unless stated otherwise, solvents used for gradient elutions were as follows. Solvent A: H_2O + 0.1% TFA; Solvent B: MeCN-H_2O 9:1 + 0.1% TFA. For HPLC control, data collection and data handling, Chromeleon software v. 6.80 was used. High resolution mass spectrometry (HRMS) was performed as matrix-assisted laser desorption/ionization time-of-flight mass spectrometry (MALDI-TOF). Analyses were performed in positive ion mode with ionization on a ThermoQExactive Orbitrap mass spectrometer (Thermo Scientific) equipped with an AP-SMALDI 10 ion source (TransmitMIT) and operated with mass resolving power 140,000 at *m/z* 200 and lock-mass for internal mass calibration. Samples were dissolved in a matrix consisting of 2,5-dihydrooxybenzoic acid (20 mg) in MeOH (1 mL). Compounds were dried under high vacuum or freeze dried using a ScanVac Cool Safe Freeze Drier.

The analysis of the ^{1}H NMR spectra was performed using the software MestReNova v12.0.0 (Mestrelab Research S.L.). Analytical hexafluoroisopropanol (HFIP) SEC was carried out at a flow rate of 0.8 mL/min at 40 °C with 3 g/L potassium trifluoroacetate added to the eluent. The SEC system was equipped with a UV detector (Jasco UV-2075 Plus) set at a wavelength of 230 nm and an RI detector (Jasco RI-2031). Modified silica gel columns (PFG columns, particle size: 7 μm, porosity: 100 and 1000 Å) were used. Molecular weights were determined by using a calibration with poly(methyl methacrylate) (PMMA) standards (Polymer Standards Service GmbH) and toluene as an internal standard. Prior to measurement, the samples were filtered through polytetrafluoroethylene (PTFE) syringe filters with a pore size of 0.2 μm. The elution diagram was analyzed with WinGPC software (Polymer Standards Service GmbH).

For the synthesis of pGlu, tetrahydrofuran (THF) and n-hexane were dried over sodium prior to use. Diethyl ether was distilled to remove the stabilizer. Dry *N*,*N*-dimethylformamide (DMF) over molecular sieves,

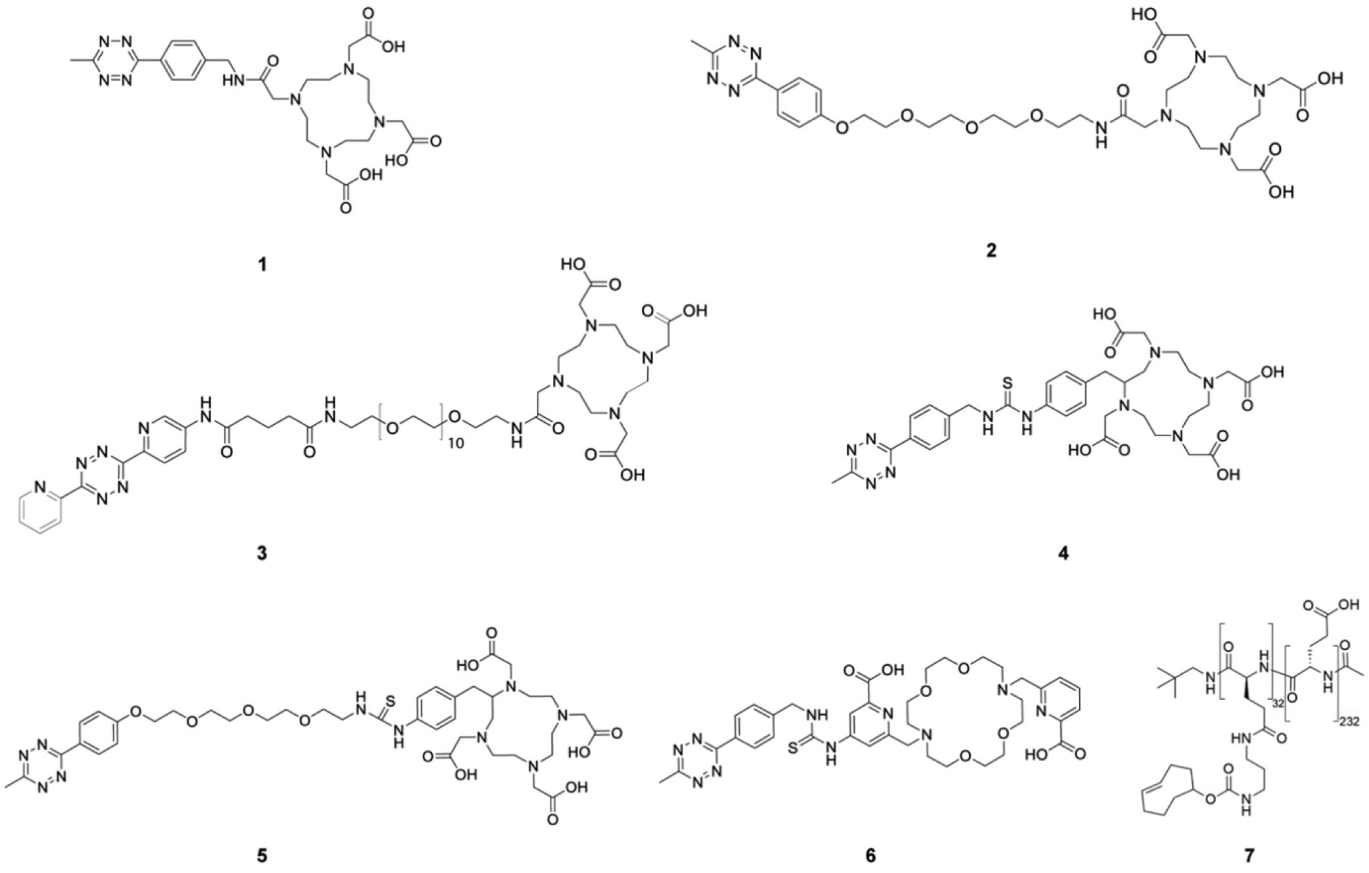

Fig. 2. Chemical structures of DOTA and macropa-modified tetrazines (Tz) and polyglutamic acid (pGlu). The constructs used in this study are heptadentate DOTA-CH_3-Tz (**1**), DOTA-PEG_4-CH_3-Tz (**2**), DOTA-PEG_{11}-BisPy-Tz (**3**), and octadentate DOTA-CH_3-Tz (**4**), DOTA-PEG_4-CH_3-Tz (**5**), decadentate macropa-Tz (**6**), and TCO-functionalized pGlu (**7**).

trifluoro-acetic acid (TFA), and hydrobromic acid were purchased from Acros. Prior to use, DMF was degassed by three freeze–pump–thaw cycles to remove residual dimethyl amine. Diphosgene was purchased from Alfa Aesar. Neopentyl-amine was purchased from TCI Europe. Isopropylamine (Sigma-Aldrich) was dried over sodium hydroxide and fractionally distilled on molecular sieves. L-Glutamic acid 5-benzyl ester was purchased from ORPEGEN Peptide Chemicals GmbH, and 2-chloro-4,6-dimethoxy-1,3,5-triazine was obtained from Carbosynth. (*E*)-Cyclooct-4-en-1-yl (3-aminopropyl) carbamate (trans-cyclooctene-amine HCl salt) was purchased from Jena Bioscience GmbH. Deuterated solvents were obtained from Deutero GmbH (Kastellaun). Milli-Q water (Millipore) with a resistance of 18.2 MΩ and TOC < 3 ppm was used throughout the experiments.

For the synthesis of Tz derivatives, (4-(6-methyl-1,2,4,5-tetrazin-3-yl) phenyl)methanamine hydrochloride salt (MeTz-NH_2) was purchased from Jena Bioscience (Germany). 2-[2-[2-[2-[4-(6-Methyl-1,2,4,5-tetrazin-3-yl)phenoxy]ethoxy]ethoxy]ethoxy]ethanamine (MeTz-PEG-NH_2) was purchased from Combi-Blocks (USA). 1,4,7,10-Tetraazacyclododecane-1,4,7,10-tetraacetic acid mono-N-hydroxysuccinimide ester (DOTA-NHS) and 2-[4,7,10-tris(carboxymethyl)-6-[(4-isothiocyanatophenyl)methyl]-1,4,7,10-tetrazacyclododec-1-yl]acetic acid (DOTA-SCN) were purchased from Macrocyclics (USA). All other chemicals and reagents were purchased from Sigma Aldrich and used without further modification unless otherwise noted. Water was purified by a Milli-Q system (Millipore, MA, USA). Phosphate buffered saline (PBS) was prepared by dissolving the tablets (Sigma-Aldrich) in MQ water. Human serum was purchased from Sigma-Aldrich.

$^{111}InCl_3$ was purchased from Curium (Oegstgeest, Netherlands).

$^{177}LuCl_3$ in 0.04 M HCl was purchased from ITG Isotope Technologies Garching GmbH (Germany). ^{225}Ac in the dry nitrate form was provided by Canadian Nuclear Laboratories (Chalk River, ON, Canada) from decay of ^{229}Th [14]. Radioactivity was measured using a CRC-55tR dose calibrator (Capintec, NJ, USA) and a gamma-ray spectrometer (Canberra GR1520) using a high purity germanium (HPGe) detector calibrated using NIST-traceable mixed ^{133}Ba and ^{152}Eu source. The dead time of the detector was kept below 10%. Quantification by gamma-ray spectrometry was performed using Canberra Genie 2000 software (v3.4, Canberra). To quantify ^{225}Ac, the gamma lines at 218 keV and 440 keV corresponding to ^{221}Fr, and ^{213}Bi, respectively were analyzed. The measurements were conducted after >5 h which is the time required to allow ^{225}Ac to reach equilibrium with its daughters (^{221}Fr and ^{213}Bi).

Radioactive thin layer chromatography (radio-TLC) was performed using silica gel 60 F254 plates (Merck) as a stationary phase and using 0.4 M sodium citrate buffer (pH 4.0) as a mobile phase on TLC scanner (Eckert & Ziegler, USA). Radioactivity on the plate was analyzed using WinScan software. Analytical radio-HPLC was performed on a Dionex system connected to a P680A pump, a UVD 170U detector, and a Scansys radiodetector. The system was controlled by Chromeleon 6.8 or Chromeleon 7.2 software.

TCO-modified pGlu (Mw = 23,300 g/mol, ~30 TCOs per polymer strand) was synthesized as previously described [49]. For the purification of radiolabeled pGlu, PD-10 desalting columns (14.5 mm × 50 mm, 8.3 mL) were used (GE Healthcare). PD10 columns were equilibrated with PBS (2 column volumes) before applying the pGlu conjugates.

2.2. Synthesis of tetrazine derivatives

2.2.1. 10-[2-[[[4-(6-Methyl-1,2,4,5-tetrazin-3-yl)phenyl]methyl]amino]-2-oxoethyl]-1,4,7,10-tetraazacyclododecane-1,4,7-triacetic acid (**1**)

A solution of MeTz-NH_2 (5.4 mg, 22.7 μmol) in anhydrous DMF (0.3 mL) was mixed with a solution of DOTA-NHS ester (18.3 mg,

24 μmol) in anhydrous DMF (0.4 mL), and triethylamine (20 μL, 143 μmol) was added to the resulting mixture. After stirring the mixture for 2.5 h at room temperature (R.T.), analytical HPLC showed the formation of a single main product. The reaction mixture was diluted with 3 volumes of water and purified by preparative HPLC (gradient conditions: 15 mL/min flow, 0–2 min, 5% B; 2–37 min, 5 → 50% B). Collected HPLC fractions containing the main product (**1**) were combined, concentrated in vacuo and lyophilized. The product was obtained as red solid (7.0 mg, 12 μmol, 52%). ^{1}H NMR (600 MHz, deuterium oxide) δ 8.43 (d, J = 8.3 Hz, 2H), 7.64 (d, J = 8.1 Hz, 2H), 4.59–4.50 (m, 2H), 4.20–3.14 (m, 28H), 3.10 (s, 3H). HRMS m/z (MALDI-TOF) calculated for $C_{26}H_{38}N_9O_7^+$: 588.2889, found: 588.2888 $[M+H]^+$. HPLC analysis and ^{1}H NMR spectrum of **1** are shown in Figs. S1 and S2, respectively.

*2.2.2. 2,2′,2″-(10-(14-(4-(6-Methyl-1,2,4,5-tetrazin-3-yl)phenoxy)-2-oxo-6,9,12-trioxa-3-azatetradecyl)-1,4,7,10-tetraazacyclododecane-1,4,7-triyl)triacetic acid (**2**)*

A solution of MeTz-PEG-NH_2 (4.8 mg, 13.2 μmol) in anhydrous DMF (0.3 mL) was mixed with a solution of DOTA-NHS ester (10.8 mg, 14.4 μmol) in anhydrous DMF (0.58 mL), and triethylamine (20 μL, 144 μmol) was added to the resulting mixture. After stirring the mixture for 2 h at R.T., analytical HPLC showed the formation of a single main product. The reaction mixture was diluted with 4 volumes of water and purified by preparative HPLC (gradient conditions: 15 mL/min flow, 0–2 min, 5% B; 2–37 min, 5 → 50% B). Collected HPLC fractions containing the main product were combined, concentrated in vacuo and lyophilized. The product (**2**) was obtained as red solid (4.6 mg, 6.1 μmol, 46%). ^{1}H NMR (600 MHz, deuterium oxide) δ 8.43 (d, J = 8.8 Hz, 2H), 7.29 (d, J = 8.9 Hz, 2H), 4.41–4.36 (m, 2H), 4.02–3.99 (m, 2H), 3.93–3.75 (m, 10H), 3.74–3.68 (m, 6H), 3.64 (t, J = 5.4 Hz, 2H), 3.57–3.12 (m, 19H), 3.07 (s, 3H). HRMS m/z (MALDI-TOF) calculated for $C_{33}H_{51}N_9O_{11}^+$: 750.3781, found: 750.3780 $[M+H]^+$. HPLC analysis and ^{1}H NMR spectrum of **2** are shown in Figs. S3 and S4, respectively.

*2.2.3. 2,2′,2″,2‴-(2-(4-(3-(4-(6-Methyl-1,2,4,5-tetrazin-3-yl)benzyl)thioureido)benzyl)-1,4,7,10-tetraazacyclododecane-1,4,7,10-tetrayl)tetraacetic acid (**4**)*

A solution of MeTz-NH_2 (4.0 mg, 16.8 μmol) in anhydrous DMF (0.5 mL) was mixed with a solution of DOTA-Bn-NCS (12.6 mg, 22.8 μmol) in anhydrous DMF (0.54 mL), and diisopropylethylamine (20 μL, 115 μmol) was added to the resulting mixture. After stirring the mixture overnight at R.T., analytical HPLC showed the formation of a single main product. The reaction mixture was diluted with 4 volumes of water and purified by preparative HPLC (purification in mobile phases containing TFA was found to lead to side product formation, so TFA in mobile phases was replaced with HCOOH, gradient conditions: 15 mL/min flow, 0–2 min, 5% B; 2–37 min, 5 → 80% B). Collected HPLC fractions containing the main product were combined, basified to apparent pH ~8 (pH strip readout) with aqueous ammonia solution, concentrated in vacuo and lyophilized. The product (**4**) was obtained as pink solid (7.0 mg, 9.3 μmol, 55%). ^{1}H NMR (600 MHz, DMSO-d_6 with 5% deuterium oxide) δ 8.42 (d, J = 7.9 Hz, 2H), 7.58 (d, J = 8.1 Hz, 2H), 7.55–7.05 (m, 4H), 4.87 (s, 2H), 4.05–2.15 (m, 27H), 2.98 (s, 3H). HRMS m/z (MALDI-TOF) calculated for $C_{34}H_{45}N_{10}O_8S^+$: 753.3137, found: 753.3136 $[M+H]^+$. HPLC analysis and ^{1}H NMR spectrum of **4** are shown in Figs. S5 and S6, respectively.

*2.2.4. 2,2′,2″,2‴-(2-(4-(3-(2-(2-(2-(2-(4-(6-Methyl-1,2,4,5-tetrazin-3-yl)phenoxy)ethoxy)ethoxy)ethoxy)ethyl)thioureido)benzyl)-1,4,7,10-tetraazacyclododecane-1,4,7,10-tetrayl)tetraacetic acid (**5**)*

A solution of MeTz-PEG-NH_2 (4.0 mg, 11 μmol) in anhydrous DMF (0.5 mL) was mixed with a solution of DOTA-Bn-NCS (8.4 mg, 15.2 μmol) in anhydrous DMF (0.36 mL), and diisopropylethylamine (20 μL, 115 μmol) was added to the resulting mixture. After stirring the mixture overnight at R.T., analytical HPLC showed the formation of a single main product. The reaction mixture was diluted with 4 volumes of water and purified by preparative HPLC (purification in mobile phases containing TFA was found to lead to side product formation, so TFA in mobile phases was replaced with HCOOH, gradient conditions: 15 mL/min flow, 0–2 min, 5% B; 2–37 min, 5 → 80% B). Collected HPLC fractions containing the main product were combined, basified to apparent pH ~8 (pH strip readout) with aqueous ammonia solution, concentrated in vacuo and lyophilized. The product (**5**) was obtained as pink solid (8.0 mg, 8.7 μmol, 79%). ^{1}H NMR (600 MHz, DMSO-d_6 with 5% deuterium oxide) δ 8.40 (d, J = 8.9 Hz, 2H), 7.53–7.00 (m, 4H), 7.20 (d, J = 9.0 Hz, 2H), 4.27–4.15 (m, 2H), 3.83–3.74 (m, 2H), 3.64–3.60 (m, 2H), 3.60–3.51 (m, 8H), 3.22 (d, J = 193.2 Hz, 29H), 2.96 (s, 3H). HRMS m/z (MALDI-TOF) calculated for $C_{41}H_{59}N_{10}O_{12}S^+$: 915.4029, found: 915.4028 $[M+H]^+$. HPLC analysis and ^{1}H NMR spectrum of **5** are shown in Figs. S7 and S8, respectively.

*2.2.5. 6-((16-((6-Carboxypyridin-2-yl)methyl)-1,4,10,13-tetraoxa-7,16-diazacyclooctadecan-7-yl)methyl)-4-(3-(4-(6-methyl-1,2,4,5-tetrazin-3-yl)benzyl)thioureido)picolinic acid (**6**)*

6-((16-((6-Carboxypyridin-2-yl)methyl)-1,4,10,13-tetraoxa-7,16-diazacyclooctadecan-7-yl)methyl)-4-isothiocyanatopicolinic acid (Macropa-NCS) was synthesized and characterized as previously described [21]. A solution of MeTz-NH_2 (1.8 mg, 4.8 μmol) in anhydrous DMF (0.18 mL) was mixed with a solution of Macropa-NHS (5 mg, 7.6 μmol) in anhydrous DMF (0.28 mL), and diisopropylethylamine (20 μL, 115 μmol) was added to the resulting mixture. After stirring the mixture for 3.5 h at R.T., analytical HPLC showed the formation of a single main product. The reaction mixture was diluted with 4 volumes of water and purified by preparative HPLC (Gemini-NX C18 preparative column, eluted with ACN in H_2O gradient, 4 mL/min, 5 to 60% ACN over 18 min, 0.25% AcOH in both). Collected HPLC fractions containing the main product were combined, concentrated in vacuo and lyophilized. The product (**6**) was obtained as purple solid (1.7 mg, 1.9 μmol, 25%). LR-ESI-MS (H_2O/MeCN 1:1) 791.2 $[M+H]^+$. HPLC analysis of **6** is shown in Fig. S9.

2,2′,2″-(10-(2,40,44-trioxo-44-((6-(6-(pyridin-2-yl)-1,2,4,5-tetrazin-3-yl)pyridin-3-yl)amino)-6,9,12,15,18,21,24,27,30,33,36-undecaoxa-3,39-diazatetratetracontyl)-1,4,7,10-tetraazacyclododecane-1,4,7-triyl) triacetic acid (**3**) was synthesized and characterized as previously described [55]. ^{1}H NMR (600 MHz, MeOD) δ 9.08 (d, J = 2.5 Hz, 1H), 8.89 (dd, J = 4.8, 0.9 Hz, 1H), 8.80–8.74 (m, 2H), 8.49 (dd, J = 8.7, 2.5 Hz, 1H), 8.18 (td, J = 7.8, 1.7 Hz, 1H), 7.74 (ddd, J = 7.6, 4.8, 1.2 Hz, 1H), 3.88–3.76 (m, 9H), 3.67–3.59 (m, 53H), 3.56 (q, J = 5.8 Hz, 5H), 3.39 (td, J = 5.5, 3.0 Hz, 5H), 2.55 (t, J = 7.3 Hz, 2H), 2.34 (t, J = 7.3 Hz, 2H), 2.04 (p, J = 7.4 Hz, 2H).

2.3. Synthesis of TCO-pGlu

Polyglutamic acid was synthesized as previously reported by Johann et al. [56]. The dispersity (Đ) of the protected pGlu(OBn) polymer was evaluated by SEC analysis and found to be 1.2 (Fig. S10). The deprotected and lyophilized polyglutamic acid sodium salt and the ((*E*)-cyclooct-4-en-1-yl(3-aminopropyl)-carbamate) (TCO) were first dissolved in water/DMSO, before the coupling agent DMTMM Cl salt was added. Afterwards the reaction was allowed to reach full. After 24 h, additional DMTMM Cl (113.0 mg) was added. Finally, the product was purified by dialysis against 6–8 kDa molecular weight cut-off (MWCO) regenerated cellulose membrane for 1 week with a daily change of water and thereafter lyophilized to obtain the final pGlu-TCO polymer. ^{1}H NMR analysis revealed a degree of polymerization of 98%, and the final TCO content was found to be 30% (Fig. S11).

2.4. Radiolabeling of tetrazines with ^{177}Lu

$^{177}LuCl_3$ in in 0.04 M HCl (1.5–3 μL, 0.3–0.7 MBq) was added to the DOTA-Tz chelates (0.01–10 nmol, 10 μL stock solution in MQ water) mixed with 0.2 M ammonium acetate buffer (87–88.5 μL, pH 6.0) and

heated at 60 °C for 10–30 min with gentle shaking. The radiochemical conversion (RCC) was determined using radio-TLC. The radio-TLC analyses were performed on silica gel plates using 0.4 M sodium citrate buffer (pH 4.0) as eluent. To quantify the radiochemical conversion (RCC), the radioactivity peaks corresponding to the Tz-bound and free unchelated ^{177}Lu radioactivity were integrated. DOTA-Tz-bound ^{177}Lu was found at $R_f = 0$, while free ^{177}Lu moved to $R_f \sim 0.5$ (Fig. S12). RCC of the Tz labeling was defined as the ratio of Tz-bound radioactivity to the sum of Tz-bound and unchelated radioactivities [57].

2.5. Radiolabeling of tetrazines with ^{225}Ac

^{225}Ac in dry nitrate form was redissolved in 4 M HNO_3 and purified with DGA as previously described [23]. ^{225}Ac (2 μL, ~100 kBq) was added to the DOTA-Tz chelates (0.01–1 nmol, 10 μL stock solution in MQ water) mixed with 0.2 M ammonium acetate buffer (88 μL, pH 6.0) and heated at 85 °C for 30–60 min with gentle shaking. Likewise, ^{225}Ac (2 μL, ~100 kBq) was added to the macropa-Tz (0.01–1 nmol, 10 μL stock solution) mixed with 0.2 M ammonium acetate buffer (88 μL, pH 6.0) and incubated at room temperature over 30 min. The RCC at 30 min and 60 min was assessed by radio-TLC on silica gel plates eluted with 0.4 M sodium citrate buffer (pH 4.0), and RCC% was quantified as described in Section 2.4.

Radio-TLC analyses were conducted at least 6 h after developing the plates to allow ^{225}Ac to reach equilibrium with its daughters (^{221}Fr and ^{213}Bi).

2.6. Estimation of accessible TCO loading of the TCO-pGlu polymer

Accessible TCO loading of the TCO-pGlu polymer was assessed by titration with ^{111}In-labeled tetrazine **3**.

The labeling of **3** with ^{111}In was performed as described previously with minor modifications [54]. Briefly, [^{111}In]$InCl_3$ in HCl was mixed with ammonium acetate buffer (pH 5.5), then **3** (2–5 nmol, 2–5 μL stock solution in MQ water) was added, and the mixture was heated at 60 °C for 5 min with gentle shaking. The radiochemical conversion was determined using radio-HPLC. Aeris Widepore C4 3.6 μm 150 × 4.6 mm column was eluted with a gradient of MeCN (solvent B) in water (solvent A) with 0.1% TFA in both solvents. Gradient conditions: 0–1 min – 5% B, 8–9 min – 75% B, 9.5–10 min – 5% B. The flow rate was set at 1.5 mL/min. Representative chromatogram of [^{111}In]**3** is shown in Fig. S13.

Aliquots of [^{111}In]**3** (20 nmol/mL solution) were mixed with aliquots of TCO-pGlu solution (0–40 μg/mL in water), incubated at room temperature for 30 min and analyzed by radio-TLC on polyethyleneimine-cellulose plates eluted with 0.1 M sodium citrate (pH 8.4). Under these conditions, [^{111}In]**3** moves to Rf ~ 0.7–0.9. The major part of [^{111}In]pGlu remains at Rf = 0, but some percentage travels to higher Rf, hence complete separation of [^{111}In]**3** from [^{111}In]pGlu is not possible. Therefore, the TCO loading of TCO-pGlu was estimated by finding the concentration of TCO-pGlu at which the fraction of radioactivity at Rf = 0 ceased to grow. This concentration results in full consumption of [^{111}In]**3**, hence the accessible concentration of TCO is 20 nmol/mL.

2.7. Radiolabeling of TCO-modified pGlu with ^{177}Lu or ^{225}Ac

TCO-modified pGlu stock solution at the concentration of 1 mg/mL (~1.3 mM TCO) was prepared in PBS. Solutions of crude ^{177}Lu or ^{225}Ac-labeled Tz derivatives (180–270 μL) were mixed with TCO-modified pGlu (20–30 μL from stock solution) and incubated at room temperature for 30 min. The molar ratio of TCO-pGlu to Tz was 10:1 and 25:1 for labeling with ^{177}Lu and ^{225}Ac, respectively.

Radiolabeled TCO-pGlu was purified by passing through PD-10 desalting column to remove the unreacted radiolabeled Tz and unchelated free radiometals. Unreacted radiolabeled DOTA-Tz and unchelated ^{177}Lu and/or ^{225}Ac were assumed to be retained on the column. PD-10 columns were eluted with PBS, two 1000 μL fractions and six 500 μL fractions were collected. The isolated radiochemical yield (RCY) was calculated as the ratio of radioactivity found in fractions 5 and 6 (both 500 μL) to the total radioactivity in all fractions collected and retained on the column (Figs. 3C and 4C) [57]. RCC of the click reaction was calculated as the ratio of the isolated RCY for [^{177}Lu/^{225}Ac]pGlu to the average RCC of the [^{177}Lu/^{225}Ac]Lu/Ac-DOTA-Tz samples used for the click reaction (Figs. 3D and 4D).

2.8. In vitro stability assay

^{177}Lu-labeled pGlu (150 μL, 40–70 kBq) or ^{225}Ac-labeled pGlu (150 μL, 5–8 kBq) was mixed with an equal volume of human serum (150 μL) and incubated at 37 °C with gentle shaking. Aliquots (10–20 μL) were withdrawn at various time points (from 1 h until seven days after the assay start) and analyzed by radio-TLC (SiO_2 plates eluted with 0.4 M citrate buffer pH 4.0). Experiments were performed in duplicate.

3. Results

3.1. TCO-pGlu reactivity toward [^{111}In]3

The accessible TCO loading of the TCO-pGlu polymer determined by the titration with [^{111}In]**3** was 0.93 nmol/μg (Fig. S14), which corresponds to 72% of the nominal TCO loading (1.29 nmol/μg) calculated from the chemical structure of the polymer.

3.2. Radiolabeling of TCO-modified pGlu with ^{177}Lu

Radiolabeling of DOTA-conjugated Tz chelates with ^{177}Lu (0.3–0.7 MBq) was optimized over a chelator concentration range from 10^{-7} to 10^{-4} M and a reaction time of 10 to 30 min using DOTA-Tz **2** as a model. Chelation RCCs increased sharply as the concentration of **2** was raised from 10^{-6} M to 10^{-4} M, while prolongation of the reaction to 30 min stabilized the RCC values (Fig. 3A). Therefore, DOTA-Tz concentration of $3 \cdot 10^{-5}$ M and reaction time of 15 min were chosen as optimal. All DOTA-Tz chelates were radiolabeled with ^{177}Lu at the optimized conditions (pH 6.0, chelator concentration of $3 \cdot 10^{-5}$ M, 15 min, 60 °C). Chelation RCCs varied from 78 ± 29% (n = 5) for [^{177}Lu]**2** to 96 ± 1% (n = 3) for [^{177}Lu]**5**. Heptadentate DOTA-Tz chelates (**1**, **2** and **3**) and octadentate ones (**4** and **5**) showed comparable RCC. We did not observe any effect of PEG linker on $^{177}Lu^{3+}$ chelation efficiency for heptadentate and octadentate chelates (Fig. 3B).

^{177}Lu-labeling of TCO-modified pGlu resulted in isolated RCYs ranging from 31% to 55% for different DOTA-Tz chelates (Fig. 3C). Calculated RCCs for the click reaction ranged from 44% to 57% (Fig. 3D). The most efficient labeling of TCO-pGlu, both in terms of isolated RCY and RCC, was achieved with [^{177}Lu]**3** (55% and 57%, respectively). For heptadentate [^{177}Lu]Lu-DOTA-Tzs **1** and **2**, the activity eluted from the PD10 column peaked in later fractions compared to other DOTA-Tz (Fig. 3E).

The radiochemical purity of all the purified ^{177}Lu-labeled pGlu were >99% as confirmed by radio-TLC.

3.3. Radiolabeling of TCO-modified pGlu with ^{225}Ac

Initial optimization of ^{225}Ac-labeling of DOTA-conjugated Tz chelates was performed using **2** as a model. In the chelator concentration screen (10^{-7}–10^{-5} M), only the highest investigated concentration gave RCC higher than 50% after 60 min reaction at 85 °C (Fig. 4A). Chelate concentration screen for the macropa-Tz 6 at ambient temperature and 30 min reaction time produced a very similar trend (Fig. 4A). Therefore, the chelate concentration for both DOTA-Tzs and macropa-Tz was fixed at 10^{-5} M. Radiolabeling of DOTA-Tzs, **1**–**5**, was then investigated at 30 and 60 min reaction time (Fig. 4B). At both reaction times, DOTA-

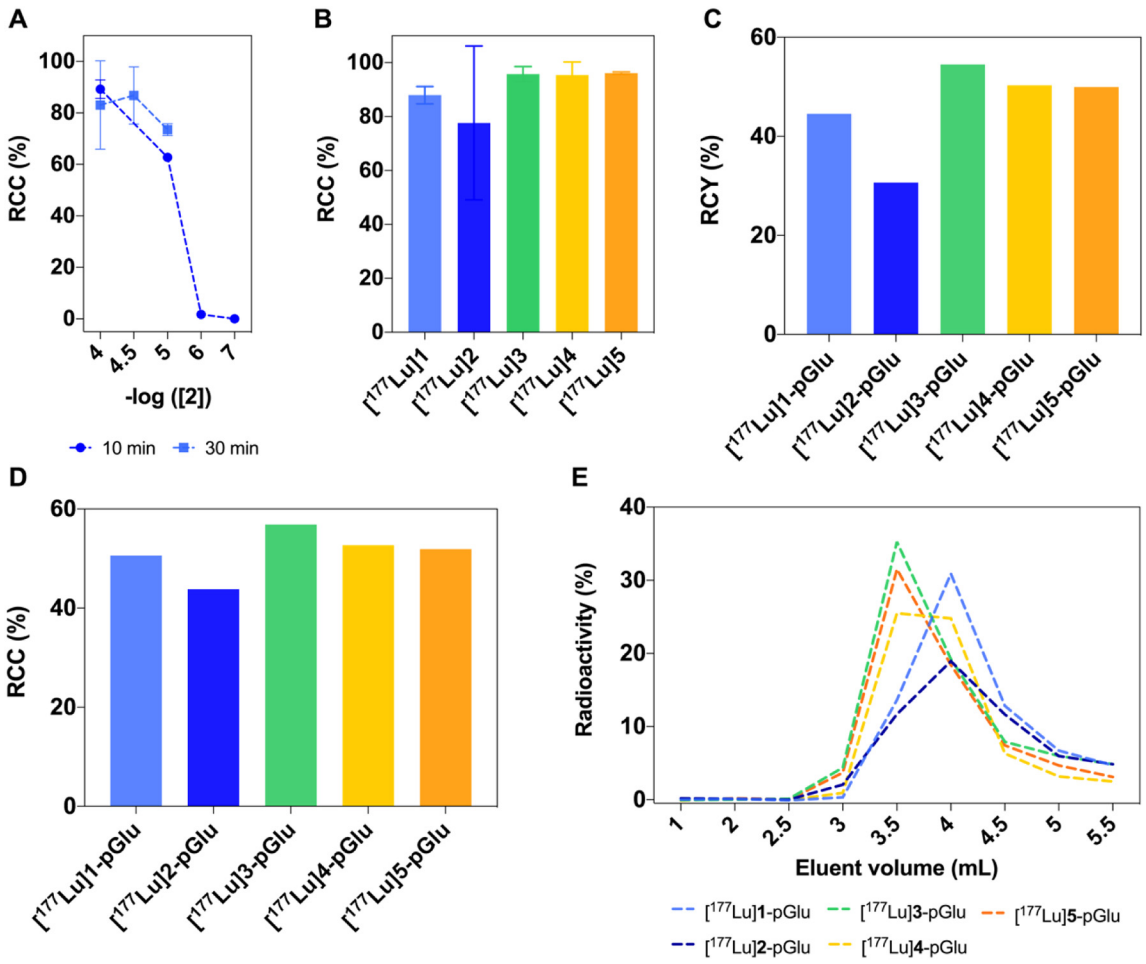

Fig. 3. Radiolabeling of TCO-functionalized pGlu with ^{177}Lu. (A) Relationship between chelation RCC (%), concentration of **2** and reaction time (n = 2). The results are reported as mean ± SD. (B) RCC (%) of DOTA-Tz chelates **1**–**5** under optimized chelation conditions (15 min reaction time, n = 3 for **1**, **3**, **4**, **5**, and n = 5 for **2**). The results are reported as mean ± SD. (C) Isolated RCY (%) of ^{177}Lu-labeled pGlu prepared with different DOTA-Tz chelates. (D) Calculated RCC (%) of the click reactions between ^{177}Lu-DOTA-Tzs and pGlu-TCO. (E) Elution profiles for ^{177}Lu-labeled pGlu. Percentage of total radioactivity collected per fraction plotted against cumulative eluent volume (mL). Radiolabeling of pGlu was performed once with each ^{177}Lu-DOTA-Tz (n = 1).

Tz derivatives with a PEG linker ([^{225}Ac]**2** and [^{225}Ac]**5**) showed lower and more variable RCCs compared to Tzs without a linker ([^{225}Ac]**1** and [^{225}Ac]**4**). Prolonging the reaction time 60 min provided more robust RCCs for [^{225}Ac]**2** (78 ± 26% at 60 min vs 48 ± 39% at 30 min) and [^{225}Ac]**5** (61 ± 34% at 60 min vs 23 ± 21% at 30 min), while the RCCs for linker-free [^{225}Ac]**1** and [^{225}Ac]**4** were nearly quantitative (Fig. 4B). Average chelation RCC for DOTA-Tz [^{225}Ac]**3** was somewhat lower at 60 min (88 ± 19%, n = 6) than at 30 min (99 ± 1%, n = 2). No considerable difference could be observed between chelation RCCs for octadentate and heptadentate DOTA-Tzs. Chelation RCC for macropa-Tz [^{225}Ac]**6** was nearly quantitative.

^{225}Ac-labeling of TCO-pGlu with methyl-Tz-DOTA chelates (**1**, **2**, **4**, and **5**) resulted in isolated RCYs of 28–51% (Fig. 4C) and calculated click RCCs of 42–76% (Fig. 4D). DOTA-Tzs with a PEG linker, [^{225}Ac]**2** and [^{225}Ac]**5**, provided higher RCCs (59% and 76%, respectively) than DOTA-Tz without a linker [^{225}Ac]**1** (RCC 52%) and [^{225}Ac]**4** (RCC 42%). However, the isolated RCYs of ^{225}Ac-pGlu were still higher for linker-free Tzs (RCCs 51%, 42%, 33% and 28% for [^{225}Ac]**1**, [^{225}Ac]**4**, [^{225}Ac]**2** and [^{225}Ac]**5**, respectively). The purification of ^{225}Ac-pGlu obtained by clicking ^{225}Ac-radiolabeled bispyridyl-Tz-DOTA, [^{225}Ac]**3**, to pGlu-TCO, produced an elution profile only marginally different from a negative control experiment using crude [^{225}Ac]**3** (Fig. 4E). Both isolated RCY and calculated click RCC equaled 20%. For [^{225}Ac]**6**-pGlu obtained from the macropa-Tz [^{225}Ac]**6**, both isolated RCY and RCC were 42%.

[^{225}Ac]**1**-pGlu, [^{225}Ac]**3**-pGlu, [^{225}Ac]**4**-pGlu, and [^{225}Ac]**6**-pGlu were obtained with radiochemical purity of >95% based on the integrity assessment by radio-TLC. The radiochemical purity of [^{225}Ac]**2**-pGlu and [^{225}Ac]**5**-pGlu were 88% and 65%, respectively.

3.4. In vitro stability of pGlu

Incubation of ^{177}Lu-labeled pGlu in 50% human serum at 37 °C showed excellent retention of the ^{177}Lu nuclide. TLC analyses detected <5% transchelation of ^{177}Lu for all ^{177}Lu-pGlu preparation over seven days with only one exception: being ^{177}Lu-pGlu-TCO prepared from DOTA-Tz [^{177}Lu]**1**, which showed ~15% unchelated ^{177}Lu on the 7th day of the incubation (Fig. 5A).

^{225}Ac-labeled pGlu, polymer conjugates prepared with DOTA-Tz [^{225}Ac]**1**, [^{225}Ac]**2**, [^{225}Ac]**3** and [^{225}Ac]**4** showed stable retention of ^{225}Ac: >90% of ^{225}Ac (>88% for [^{225}Ac]**2**-pGlu) remained chelated over six days. pGlu labeled with [^{225}Ac]**5** contained only 72% chelated ^{225}Ac at the start of the incubation, but did not decrease over the course of the assay. [^{225}Ac]**6**-labeled pGlu contained virtually no free ^{225}Ac at the beginning of the assay but showed a steady release of ^{225}Ac over the course of the incubation – up to 37% after six days (Fig. 5B).

4. Discussion

In this study, we report the radiolabeling of chelator-modified Tzs with therapeutic radioisotopes ^{177}Lu and ^{225}Ac and their subsequent use for the preparation of ^{177}Lu and ^{225}Ac-labeled polypeptide pGlu via Tz-TCO ligation. The radionuclide ^{225}Ac has gained increasing

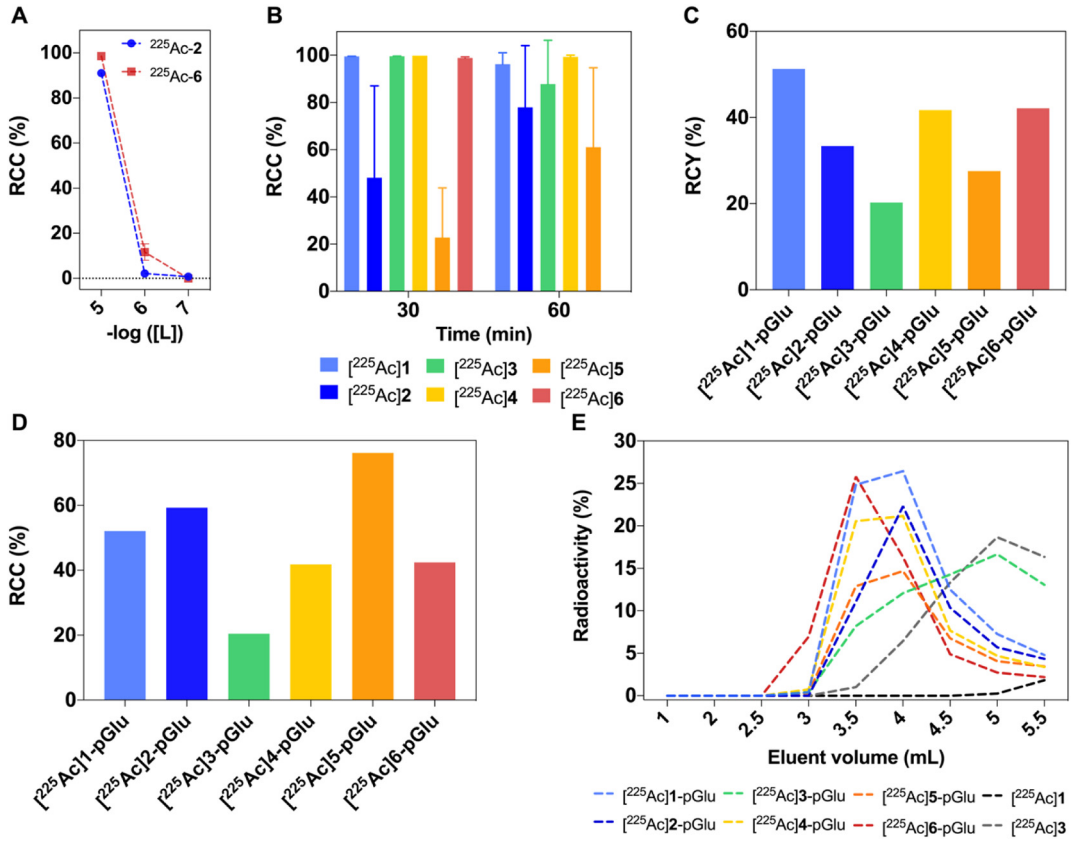

Fig. 4. Radiolabeling of TCO-functionalized pGlu with ^{225}Ac. (A) Relationship between chelation RCC (%), concentration of **2** or **6** and reaction time (n = 2). The results are reported as mean ± SD. (B) RCC (%) of Tz chelates at 10^{-5} M concentration, 85 °C (**1**–**5**) or ambient temperature (**6**) and reaction time of 30 and 60 min. The results are reported as mean ± SD. (C) Isolated RCY (%) of ^{225}Ac-labeled pGlu prepared with different chelates. (D) Calculated RCC (%) of the click reactions between ^{225}Ac-labeled Tzs and pGlu-TCO. (E) Elution profiles for ^{225}Ac-labeled pGlu. Percentage of total radioactivity collected per fraction plotted against cumulative eluent volume (mL). Radiolabeling of pGlu was performed once with each ^{225}Ac-Tz (n = 1).

attention due to its decay characteristics and successful clinical results of ^{225}Ac-PSMA-617 for treating advanced, metastatic castrate-resistant prostate cancer [58,59]. ^{225}Ac-labeled immunoconjugates were previously synthesized using a similar approach for targeted alpha radioimmunotherapy by Poty et al. [35]. However, the use of Tz-TCO ligation for ^{177}Lu and ^{225}Ac labeling of engineered polymers, which could be used as radiopharmaceuticals for radionuclide therapy, has not been reported so far. TCO-functionalized pGlu polymer used in this study was previously shown to have excellent tumor retention upon intratumoral injection [49]. Similar TCO-functionalized pGlu polymers, with pSar strands grafted onto the pGlu backbone, showed highly efficient EPR-mediated tumor targeting [50].

An important advantage of engineered polymers over antibodies is that the number of TCO groups can be varied more widely to control the IEDDA ligation kinetics and radionuclide load [60]. For example, Rossin et al. demonstrated that increased hydrophobicity resulting from extensive TCO-modification of the antibody CC49 was detrimental to its performance in IEDDA-based pretargeting [61]. Furthermore, additional functionalities on pGlu could allow for multimodal imaging and theranostic applications [62–67]. In this work we deliberately used an excess of TCO-pGlu (10–25-fold) relative to chelator-Tz in order to leave most of TCO moieties intact. These extra TCOs can be used to attach imaging probes or extra therapeutic payload for combination therapy either before the intratumoral injection or after it by means of pretargeting. For

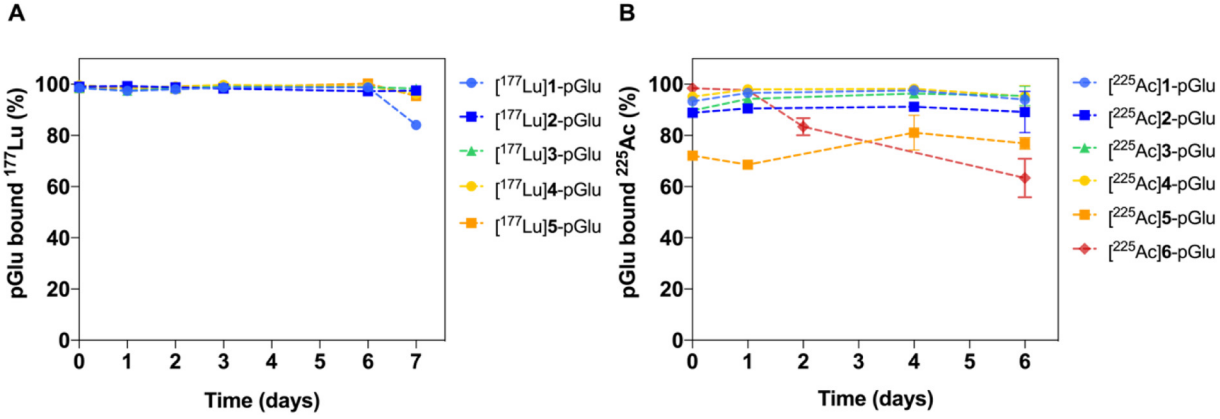

Fig. 5. *In vitro* stability of ^{177}Lu-pGlu (A) and ^{225}Ac-pGlu (B) in human serum based on radio-TLC analysis. The experiments were performed in duplicate and are reported as mean ± SD.

example, Tz-drug conjugates releasing drugs upon TCO-Tz click are already known [68].

Almost all DOTA-modified Tz derivatives efficiently chelated ^{177}Lu resulting in average RCC of >80% (Fig. 3B). The lowest average RCC was observed for [^{177}Lu]2 (78 ± 29%, n = 5), which is more likely the result of greater RCC variance that manifested itself when more independent labeling experiments were performed. Heptadentate (**1**–**3**) and octadentate (**4**–**5**) DOTA-Tzs showed comparable chelation RCCs.

Isolated RCYs for ^{177}Lu-labeled pGlu-TCO conjugates were 40% or more for 4 out of 5 investigated [^{177}Lu]Lu-DOTA-Tzs (Fig. 3C). Calculated RCCs for the click reactions between crude [^{177}Lu]Lu-DOTA-Tzs and pGlu-TCO polymer were on the order of 50%, i.e. only half of the chelated ^{177}Lu radioactivity could be isolated in the form of ^{177}Lu-labeled polymer (Fig. 3D). This might be evidence of partial loss of click reactivity by the DOTA-Tzs during the labeling, but is possibly also due to insufficient recovery of the pGlu-TCO polymer from the PD10 sorbent. [^{177}Lu]**3** showed the most efficient conjugation to TCO-pGlu among ^{177}Lu-labeled DOTA-Tz chelates used in this study.

The RCCs for ^{225}Ac chelation by DOTA-Tzs (Fig. 4B) were lower and more variable than for ^{177}Lu chelation. This can be due to ^{225}Ac being more difficult to chelate than ^{177}Lu and to the fact that the DOTA-Tz concentration selected for ^{225}Ac experiments was 3-fold lower than the concentration used for ^{177}Lu experiments ($1 \cdot 10^{-5}$ M and $3 \cdot 10^{-5}$ M, respectively). In particular, chelation RCCs for DOTA-Tzs with a PEG linker (**2** and **5**) were considerably lower than for structurally related linker-free DOTA-Tzs (**1** and **4**, Fig. 4B). One could argue that, contrary to our expectations before the study, the PEG chain in **2** and **5** might sterically hinder the chelation of ^{225}Ac by DOTA instead of preserving its chelating properties by moving the Tz moiety farther away. However, DOTA-Tz **3**, with a much longer PEG linker compared to **2** and **5**, showed chelation RCCs similar to **1** and **4**. In contrast to DOTA-Tzs, macropa-Tz (**6**) showed excellent chelation of ^{225}Ac at ambient temperature after 30 min (RCC of >98%). Macropa maintains a large macrocyclic cavity suitable for the $^{225}Ac^{3+}$ ion (1.12 Å; CN = 6) and was reported to be a highly promising chelate compared to DOTA [21,69].

As a consequence of lower chelation RCCs for ^{225}Ac compared to ^{177}Lu, isolated RCYs of ^{225}Ac-labeled pGlu-TCO conjugates exceeded 40% for only 3 out of 6 ^{225}Ac-labeled chelator-Tzs (Fig. 4C). As with [^{177}Lu]Lu-DOTA-Tzs, only about half of the chelated ^{225}Ac activity, on average, could be isolated as ^{225}Ac-labeled polymer. An outlier in this regard was [^{225}Ac]**3**, which showed click RCC of only 20% (Fig. 4D), despite having an almost quantitative chelation RCC. One possible explanation of this finding is that [^{225}Ac]**3** could become partially decomposed and lose its click reactivity during prolonged incubation at high temperature (60 min at 85 °C) required for ^{225}Ac chelation of DOTA. This explanation is indirectly supported by previous studies, where bispyridyl-Tzs such as **3** was reported to be more reactive but less stable compared to methyl-Tzs such as **1**, **2**, **4** and **5** [70]. Another explanation could be that [^{225}Ac]**3**, having a relatively high molecular weight (~2 kDa), could not be efficiently separated from the corresponding [^{225}Ac]**3**-pGlu conjugate by the PD10 column. Another outlier is [^{225}Ac]**5**, which showed an unusually high click RCC (76%, Fig. 4D), but the purified [^{225}Ac]**5**-pGlu conjugate was later found to contain 28% unchelated ^{225}Ac. Summing up, PD10 column purification did not work well enough for the isolation of [^{225}Ac]**3**-pGlu and [^{225}Ac]**5**-pGlu conjugates.

All ^{177}Lu-labeled pGlu conjugates showed excellent stability in plasma – less than 5% unchelated ^{177}Lu over six days (Fig. 5A). For ^{225}Ac-labeled pGlu prepared from linker-free DOTA-Tzs ([^{225}Ac]**1**-pGlu and [^{225}Ac]**4**-pGlu), as well as for [^{225}Ac]**3**-pGlu prepared from the extra-long-linker DOTA-Tz, [^{225}Ac]**3**, unchelated ^{225}Ac content stayed below 10% over six days of incubation (Fig. 5B). For another DOTA-Tz with a PEG linker, [^{225}Ac]**2**, the corresponding pGlu conjugate was less pure (~12% unchelated ^{225}Ac), but did not release any more ^{225}Ac during the incubation in plasma. For the DOTA-Tz conjugate with the highest content of unchelated ^{225}Ac, [^{225}Ac]**5**-pGlu, no further degradation could be detected throughout the duration of the stability assay. Thus, there seemed to be no difference between the stability of heptadentate and octadentate DOTA complexes of ^{177}Lu and ^{225}Ac. [^{225}Ac]**6**-pGlu conjugate prepared from the macropa-Tz [^{225}Ac]**6** showed measurable loss of ^{225}Ac activity over six days in plasma, with unchelated ^{225}Ac content reaching 37% on day 6 (Fig. 5B). Therefore, although the macropa chelator showed efficient ^{225}Ac chelation at much milder labeling conditions compared to DOTA, its ability to retain ^{225}Ac was clearly inferior to DOTA in our study.

5. Conclusion

We investigated the radiolabeling of the chelator-modified Tz derivatives with ^{177}Lu and ^{225}Ac, and their IEDDA conjugations to TCO-modified pGlu. Efficient chelation of ^{177}Lu (RCC > 80%) was achieved with all DOTA-modified Tz derivatives except one. Efficient chelation of ^{225}Ac was achieved with linker-free DOTA-Tz derivatives (**1** and **4**) as well as with macropa-Tz **6**. The latter did not require heating for the chelation of ^{225}Ac. No difference in chelation efficiency between heptadentate and octadentate DOTA were observed.

Conjugation of ^{177}Lu and ^{225}Ac labeled Tzs produced radiolabeled polymer conjugates in acceptable RCYs of up to 55% (over two steps). Radiolabeled ^{177}Lu-pGlu conjugates obtained from all DOTA-Tzs and ^{225}Ac-pGlu conjugates obtained from linker-free DOTA-Tzs showed excellent stability in human plasma.

The results obtained herein are promising and indicate the advantage of using Tz-TCO ligation for the radiolabeling of pGlu with ^{177}Lu and ^{225}Ac. Further *in vitro* cell uptake and *in vivo* evaluation of the prepared ^{177}Lu-pGlu and ^{225}Ac-pGlu conjugates are being planned in order to demonstrate their value as radiotherapeutic agents.

Abbreviations

DOTA	1,4,7,10-Tetraazacyclododecane-1,4,7,10-tetraacetic acid
IEDDA	Inverse electron-demand Diels–Alder
macropa	*N*, *N*′-bis[(6-carboxy-2-pyridil)]-4, 13-diaza-18-crown-6
PEG	Polyethylene glycol
pGlu	Polyglutamate
RCC	Radiochemical conversion
RCY	Radiochemical yield
TCO	Trans-cyclooctene
Tz	Tetrazine

CRediT authorship contribution statement

VS, MMH, and VR conceptualized the study. KJ and MB prepared and characterized the TCO-pGlu polymer. VS performed the radiochemical synthesis and labeling experiments. VS and GE analyzed the data. LW and GE performed some of the ^{225}Ac-labeling experiments and characterized the synthesized macropa-Tz chelator. GE wrote the first draft, VS and LB edited the draft, and all authors revised and approved the manuscript.

Declaration of competing interest

The authors declare no competing interests.

Acknowledgements

TRIUMF receives funding via a contribution agreement with the National Research Council Canada. We would like to thank Dr's Patrick Causey, Randy Perron and Denise Gendron (Canadian Nuclear Laboratories, ON, Canada) for providing purified ^{225}Ac for radiolabeling studies. VS was supported by the Lundbeck Foundation, grant number R303-2018-3567. This work was supported through the NSERC Discovery Grant (RGPIN-2018-04997 (VR)), from the Natural Sciences

and Engineering Research Council of Canada. We also would like to thank Prof. Justin Wilson (Cornell University, Ithaca, NY, USA) for providing macropa-NCS and Prof. Chris Orvig and Prof. Urs Hafeli (University of British Columbia, Vancouver, BC, Canada) for their support.

Appendix A. Supplementary data

Supplementary data to this article can be found online at https://doi.org/10.1016/j.nucmedbio.2021.11.001.

References

[1] Volkert WA, Hoffman TJ. Therapeutic radiopharmaceuticals. Chem Rev. 1999;99(9):2269–92.
[2] Sgouros G, et al. Radiopharmaceutical therapy in cancer: clinical advances and challenges. Nat Rev Drug Discov. 2020;19(9):589–608.
[3] Tanderup K, et al. Advancements in brachytherapy. Adv Drug Deliv Rev. 2017;109:15–25.
[4] Banerjee S, Pillai MRA, Knapp FF. Lutetium-177 therapeutic radiopharmaceuticals: linking chemistry, radiochemistry, and practical applications. Chem Rev. 2015;115(8):2934–74.
[5] Milenic DE, Brady ED, Brechbiel MW. Antibody-targeted radiation cancer therapy. Nat Rev Drug Discov. 2004;3(6):488–99.
[6] Koppe MJ, et al. Biodistribution and therapeutic efficacy of (125/131)I-, (186)Re-, (88/90)Y-, or (177)Lu-labeled monoclonal antibody MN-14 to carcinoembryonic antigen in mice with small peritoneal metastases of colorectal origin. J Nucl Med. 2004;45(7):1224–32.
[7] Hennrich U, Kopka K. Lutathera((R)): the first FDA- and EMA-approved radiopharmaceutical for peptide receptor radionuclide therapy. Pharmaceuticals (Basel). 2019;12(3).
[8] Hatcher-Lamarre JL, et al. Alpha emitting nuclides for targeted therapy. Nucl Med Biol. 2021;92:228–40.
[9] Kim YS, Brechbiel MW. An overview of targeted alpha therapy. Tumour Biol. 2012;33(3):573–90.
[10] Elgqvist J, et al. The potential and hurdles of targeted alpha therapy - clinical trials and beyond. Front Oncol. 2014;3:324.
[11] Kratochwil C, Haberkorn U, Giesel FL. (225)Ac-PSMA-617 for therapy of prostate cancer. Semin Nucl Med. 2020;50(2):133–40.
[12] Ferrier MG, Radchenko V, Wilbur DS. Radiochemical aspects of alpha emitting radionuclides for medical application. Radiochim Acta. 2019;107(9–11):1065–85.
[13] Robertson AKH, et al. Development of (225)Ac radiopharmaceuticals: TRIUMF perspectives and experiences. Curr Radiopharm. 2018;11(3):156–72.
[14] Perron R, Gendron D, Causey PW. Construction of a thorium/actinium generator at the Canadian Nuclear Laboratories. Appl Radiat Isot. 2020;164:109262.
[15] Robertson AKH, et al. (232)Th-spallation-produced (225)Ac with reduced (227)Ac content. Inorg Chem. 2020;59(17):12156–65.
[16] Kostelnik TI, Orvig C. Radioactive main group and rare earth metals for imaging and therapy. Chem Rev. 2019;119(2):902–56.
[17] National Nuclear Data Center. Nudat2. NY (USA): Brookhaven National Laboratory; 2004.
[18] McDevitt MR, et al. Design and synthesis of 225Ac radioimmunopharmaceuticals. Appl Radiat Isot. 2002;57(6):841–7.
[19] Cortez A, et al. Evaluation of [(225)Ac]Ac-DOTA-anti-VLA-4 for targeted alpha therapy of metastatic melanoma. Nucl Med Biol. 2020;88–89:62–72.
[20] Chappell LL, et al. Synthesis, conjugation, and radiolabeling of a novel bifunctional chelating agent for (225)Ac radioimmunotherapy applications. Bioconjug Chem. 2000;11(4):510–9.
[21] Thiele NA, et al. An eighteen-membered macrocyclic ligand for actinium-225 targeted alpha therapy. Angew Chem Int Ed Engl. 2017;56(46):14712–7.
[22] Li L, et al. (225)Ac-H4py4pa for targeted alpha therapy. Bioconjug Chem. 2021;32(7):1348–63.
[23] Yang H, et al. Synthesis and evaluation of a macrocyclic actinium-225 chelator, quality control and in vivo evaluation of (225) Ac-crown-alphaMSH peptide. Chemistry. 2020;26(50):11435–40.
[24] Zeglis BM, et al. A pretargeted PET imaging strategy based on bioorthogonal Diels-Alder click chemistry. J Nucl Med. 2013;54(8):1389–96.
[25] Zeglis BM, et al. Optimization of a pretargeted strategy for the PET imaging of colorectal carcinoma via the modulation of radioligand pharmacokinetics. Mol Pharm. 2015;12(10):3575–87.
[26] Denk C, et al. Design, synthesis, and evaluation of a low-molecular-weight (11)C-labeled tetrazine for pretargeted PET imaging applying bioorthogonal in vivo click chemistry. Bioconjug Chem. 2016;27(7):1707–12.
[27] Houghton JL, et al. Establishment of the in vivo efficacy of pretargeted radioimmunotherapy utilizing inverse electron demand Diels-Alder click chemistry. Mol Cancer Ther. 2017;16(1):124–33.
[28] Poty S, et al. Leveraging bioorthogonal click chemistry to improve (225)Ac-radioimmunotherapy of pancreatic ductal adenocarcinoma. Clin Cancer Res. 2019;25(2):868–80.
[29] Membreno R, et al. Toward the optimization of click-mediated pretargeted radioimmunotherapy. Mol Pharm. 2019;16(5):2259–63.
[30] Zeglis BM, et al. Modular strategy for the construction of radiometalated antibodies for positron emission tomography based on inverse electron demand Diels-Alder click chemistry. Bioconjug Chem. 2011;22(10):2048–59.
[31] Canovas C, et al. Modular assembly of multimodal imaging agents through an inverse electron demand Diels-Alder reaction. Bioconjug Chem. 2019;30(3):888–97.
[32] Selvaraj R, et al. Tetrazine-trans-cyclooctene ligation for the rapid construction of integrin alphavbeta(3) targeted PET tracer based on a cyclic RGD peptide. Bioorg Med Chem Lett. 2011;21(17):5011–4.
[33] Litau S, et al. iEDDA conjugation reaction in radiometal labeling of peptides with (68)Ga and (64)Cu: unexpected findings. ACS Omega. 2018;3(10):14039–53.
[34] Blackman ML, Royzen M, Fox JM. Tetrazine ligation: fast bioconjugation based on inverse-electron-demand Diels-Alder reactivity. J Am Chem Soc. 2008;130(41):13518–9.
[35] Poty S, et al. The inverse electron-demand Diels-Alder reaction as a new methodology for the synthesis of (225)Ac-labelled radioimmunoconjugates. Chem Commun (Camb). 2018;54(21):2599–602.
[36] Hruby M, et al. Thermoresponsive polymeric radionuclide delivery system–an injectable brachytherapy. Eur J Pharm Sci. 2011;42(5):484–8.
[37] Schaal JL, et al. Injectable polypeptide micelles that form radiation crosslinked hydrogels in situ for intratumoral radiotherapy. J Control Release. 2016;228:58–66.
[38] Sano K, et al. Brachytherapy with intratumoral injections of radiometal-labeled polymers that thermoresponsively self-aggregate in tumor tissues. J Nucl Med. 2017;58(9):1380–5.
[39] Phillips WT, et al. Rhenium-186 liposomes as convection-enhanced nanoparticle brachytherapy for treatment of glioblastoma. Neuro Oncol. 2012;14(4):416–25.
[40] Wang W, et al. Preclinical evaluation of cationic DOTA-triarginine-lipid conjugates for theranostic liquid brachytherapy. Nanotheranostics. 2020;4(3):142–55.
[41] Fach M, et al. Effective intratumoral retention of [(103) Pd]AuPd alloy nanoparticles embedded in gel-forming liquids paves the way for new nanobrachytherapy. Adv Healthc Mater. 2021;10(10):e2002009.
[42] Yook S, et al. Intratumorally injected 177Lu-labeled gold nanoparticles: gold nanoseed brachytherapy with application for neoadjuvant treatment of locally advanced breast cancer. J Nucl Med. 2016;57(6):936–42.
[43] Barz M, et al. Overcoming the PEG-addiction: well-defined alternatives to PEG, from structure-property relationships to better defined therapeutics. . 2011;2:1900–18.
[44] Schafer O, et al. Investigation of a-amino acid N-carboxyanhydrides by X-ray diffraction for controlled ring-opening polymerization. Tetrahedron Lett. 2019;60:272–5.
[45] Yin L, et al. Synthetic polypeptides for drug and gene delivery, and tissue engineering. Adv Drug Deliv Rev. 2021;178:113995.
[46] Patravale V, Dandekar P, Jain R. Clinical trials industrial aspects. Nanoparticulate drug delivery. Perspectives on the transition from laboratory to market. Woodhead Publishing Limited; 2012. p. 191–207.
[47] Meyers JD, et al. Nanoparticles for imaging and treating brain cancer. Nanomedicine (Lond). 2013;8(1):123–43.
[48] Barz M, Duro-Castano A, Vicent MJ. A versatile post-polymerization modification method for polyglutamic acid: synthesis of orthogonal reactive polyglutamates and their use in “click chemistry”. . 2013;4:2989–94.
[49] Steen EJL, et al. Improved radiosynthesis and preliminary in vivo evaluation of the (11)C-labeled tetrazine [(11)C]AE-1 for pretargeted PET imaging. Bioorg Med Chem Lett. 2019;29(8):986–90.
[50] Steen EJL, et al. Trans-cyclooctene-functionalized PeptoBrushes with improved reaction kinetics of the tetrazine ligation for pretargeted nuclear imaging. ACS Nano. 2020;14(1):568–84.
[51] Rossin R, et al. Diels-Alder reaction for tumor pretargeting: in vivo chemistry can boost tumor radiation dose compared with directly labeled antibody. J Nucl Med. 2013;54(11):1989–95.
[52] van Duijnhoven SM, et al. Diabody pretargeting with click chemistry in vivo. J Nucl Med. 2015;56(9):1422–8.
[53] Edem PE, et al. EJNMMI Res. 2019;9(1):49.
[54] Edem PE, et al. Evaluation of a (68)Ga-labeled DOTA-tetrazine as a PET alternative to (111)In-SPECT pretargeted imaging. Molecules. 2020;25(3).
[55] Poulie CBM, et al. Evaluation of [(64)Cu]Cu-NOTA-PEG7-H-tz for pretargeted imaging in LS174T xenografts-comparison to [(111)In]In-DOTA-PEG11-BisPy-tz. Molecules. 2021;26(3).
[56] Johann K, et al. Tetrazine- and trans-cyclooctene-functionalised polypept(o)ides for fast bioorthogonal tetrazine ligation. . 2020;11:4396–407.
[57] Herth MM, et al. On the consensus nomenclature rules for radiopharmaceutical chemistry - reconsideration of radiochemical conversion. Nucl Med Biol. 2021;93:19–21.
[58] Kratochwil C, et al. 225Ac-PSMA-617 for PSMA-targeted alpha-radiation therapy of metastatic castration-resistant prostate cancer. J Nucl Med. 2016;57(12):1941–4.
[59] Kratochwil C, et al. Targeted alpha-therapy of metastatic castration-resistant prostate cancer with (225)Ac-PSMA-617: swimmer-plot analysis suggests efficacy regarding duration of tumor control. J Nucl Med. 2018;59(5):795–802.
[60] Steen EJL, et al. Pretargeting in nuclear imaging and radionuclide therapy: improving efficacy of theranostics and nanomedicines. Biomaterials. 2018;179:209–45.
[61] Rossin R, et al. Trans-cyclooctene tag with improved properties for tumor pretargeting with the Diels-Alder reaction. Mol Pharm. 2014;11(9):3090–6.
[62] Tanisaka H, et al. Near-infrared fluorescent labeled peptosome for application to cancer imaging. Bioconjug Chem. 2008;19(1):109–17.
[63] Adumeau P, et al. A pretargeted approach for the multimodal PET/NIRF imaging of colorectal cancer. Theranostics. 2016;6(12):2267–77.
[64] Xie X, et al. Bioorthogonal nanosystem for near-infrared fluorescence imaging and prodrug activation in mouse model. . 2019;1(5):549–57.
[65] Goos J, et al. Design and preclinical evaluation of nanostars for the passive pretargeting of tumor tissue. Nucl Med Biol. 2020;84–85:63–72.
[66] Dong Y, et al. A general strategy for macrotheranostic prodrug activation: synergy between the acidic tumor microenvironment and bioorthogonal chemistry. Angew Chem Int Ed Engl. 2020;59(18):7168–72.

[67] Keinanen O, et al. Harnessing (64)Cu/(67)Cu for a theranostic approach to pretargeted radioimmunotherapy. Proc Natl Acad Sci U S A. 2020;117(45):28316–27.
[68] van Onzen A, et al. Bioorthogonal tetrazine carbamate cleavage by highly reactive trans-cyclooctene. J Am Chem Soc. 2020;142(25):10955–63.
[69] Thiele NA, Wilson JJ. Actinium-225 for targeted alpha therapy: coordination chemistry and current chelation approaches. Cancer Biother Radiopharm. 2018;33(8):336–48.
[70] Oliveira BL, Guo Z, Bernardes GJL. Inverse electron demand Diels-Alder reactions in chemical biology. Chem Soc Rev. 2017;46(16):4895–950.